Received: 9 December 2020 | Revised: 24 February 2021 | Accepted: 3 March 2021

DOI: 10.1111/1556-4029.14705

JOURNAL OF FORENSIC SCIENCES

PAPER

Questioned Documents

Determining the chronological sequence of inks deposited with different writing and printing tools using ion beam analysis

Vairavel Mathayan PhD[1] | Mauricio Sortica PhD[2] | Daniel Primetzhofer PhD[1,2]

[1]Department of Physics and Astronomy, Uppsala University, Uppsala, Sweden

[2]Tandem Laboratory, Uppsala University, Uppsala, Sweden

Correspondence
Vairavel Mathayan, Department of Physics and Astronomy, Uppsala University, Box 516, SE-75120 Uppsala, Sweden.
Email: vairavel.mathayan@physics.uu.se

Funding information
Accelerator operation was supported by Swedish Research Council VR-RFI (Contract No. 2017-00646_9) and the Swedish Foundation for Strategic Research (Contract No. RIF14-0053).

Abstract

Determining the sequence of inks in a questioned document is important in forensic science. Conventional and micro beam-based ion beam analysis using Rutherford backscattering spectrometry (RBS) and particle-induced X-ray emission were employed to study the depth distribution of chemical elements in plain paper and inks/toner deposited by different pens as well as inkjet and laser printers. Composition depth profiling with high lateral resolution was performed with focus on areas where two different coloring agents overlapped. We identify under which conditions the sequence of inks deposited can be reconstructed, analyzing the continuity of characteristic contributions to the obtained signals, with a focus on the depth-resolved RBS data. The order of deposition was correctly determined for combinations of two different laser printers and in certain cases for pens. Results indicate a potential for analysis, depending on the composition of staining agent, that is, in particular if heavy species are present in sufficiently high concentration. In such cases, also characters obscured or modified by an agent of different composition can be revealed. Changing the probing depth by modifying the beam energy could yield additional information.

KEYWORDS
ink composition, ink discrimination, particle-induced X-ray emission, Rutherford backscattering spectrometry, sequence of inks

Highlights

- Composition depth profiling of paper and different inks by Rutherford Backscattering Spectrometry.
- Potential of ion beam analysis for forensic analysis of printed and/or written documents is assessed.
- Mapping by Rutherford Backscattering Spectrometry (RBS) and particle-induced X-ray emission (PIXE).
- Deposition sequence in documents with overlapping lines can be determined in some cases.
- Near-surface deposition and presence of heavy elements in staining agents increases success rate.

1 | INTRODUCTION

Determining the deposition sequence of inks, that is, if a questioned document is a document with overlapping lines from, for example, signatures and print, or possibly multiple printing instances, finding the first printed ink can be useful to identify forged documents. Many methods have been employed to find the order of deposition of inks in documents due to its importance in forensic investigations [1]. In particular, optical methods using light microscopes have been used for identifying the sequence of inks in a document. In these methods, authors used various interpretations and methodologies, that is, ink investigations using reflected light, grazing light, and transmitted light [1,2]; thus optical methods need a trained expert for analysis, and results may be of qualitative character. Raman spectroscopy and Raman imaging techniques have been used for discriminating inks and finding the sequence of inks in a questioned document [3–5]. Near-infrared hyperspectral imaging has been applied for predicting forgery in a document prepared by different pens and this method correctly predicted 17 out of 20 samples [6]. Mass spectrometry imaging using easy ambient sonic-spray ionization has been used to find the sequence of inks at intersection of stamp and pen ink [7]. Atomic force microscopy has been used to measure height profiles of inks deposited on paper, and the sequence of inks has been predicted by the height profiles at the intersection [8]. Many other methods have been reported to be capable to determine the chronological deposition order inks on paper, such as using adhesive taps [9], FTIR spectroscopy [10], laser desorption ionization mass spectrometry (LDI-MS) [11], and scanning electron microscope [12].

Recently, ion beam analytical techniques, in particular MeV secondary ion mass spectrometry (MeV-SIMS) and particle-induced X-ray emission (PIXE), have been used for forensic analysis of inks/laser toners deposited on the documents. The order of ink deposition was identified by the presence of a gap at the ink distribution map, for example, the ink deposited first showed a gap or discontinuity at the crossing and the ink deposited on top showing continuity [13–16].

As a complement to these earlier studies highlighting the potential of some ion beam-based tools for forensic analysis of documents, in this study, we assess the potential of Rutherford backscattering spectrometry (RBS) to identify the deposition sequence of different inks from pens and printers as well as printer toners. Different from PIXE, which is superior in sensitivity for heavy elements, Rutherford backscattering spectrometry enables straightforward and quantitative depth profiling of materials [17]. As such the method provides a powerful tool for thickness and composition analysis of bulk and thin film samples down to a few μm depth from the sample surface, primarily used for materials science [18], but has also shown its potential for analysis of organic systems containing traces of heavy elements [19]. Specifically, in our present study, combined micro-RBS and micro-PIXE mapping is performed at the intersection of two different inks (laser toner, inkjet ink, ballpoint pen, and gel pen). The results are correlated with the deposition sequence of the inks present on the document.

2 | MATERIALS AND METHODS

Conventional RBS and micro-RBS were performed on the inks deposited by printing and writing tools. All ion beam experiments were performed at the tandem laboratory, Uppsala University, employing a 5 MV pelletron accelerator. For obtaining reference spectra using RBS and PIXE, the inks (described in Table 1) were homogeneously deposited on paper. Conventional RBS was performed employing a beam of 2 MeV He^+ primary ions and using a silicon-solid state detector (SSD) kept at 170° scattering angle. Simultaneously, PIXE data

TABLE 1 Composition of paper and inks used in the documents

Paper/writing tool	Color	Ink name	Composition from RBS (at.%)
Plain paper	—	—	C(64), N(~3), O(25), Na(~2), Si(<1), P(<1), S(<1), Cl(<1), Ca (~5)
HP LaserJet 1010-laser printer	Black	Laser print 1	C(72), N(~2), O(18), Na(<1), Si(<1), P(<1), S(<1), Cl(<1), Ca (<1), Fe(~7)
Ricoh mp c307 -Laser printer	Black	Laser print 2	C(77), N(~2), O(16), Na(~2), Si(~1), P(<1), S(<1), Cl(<1), Ca (~1)
Canon pixma ix6820 inkjet printer	Black	Ink jet	C(70), N(~3), O(20), Na(~2), Si(<1), P(<1), S(<1), Cl(<1), Ca (~3)
Foray Rollerball Pen Comfort Gel	Black	Gel pen	C(74), N(~2), O(17), Na(~3), Si(~1), P(<1), S(<1), Cl(<1), Ca (~3)
Ballograf ballpoint pen	Blue	Ball-point pen	C(66), N(~6), O(21), Na(~3), Si(<1), P(<1), S(<1), Cl(<1), Ca (~3)

were recorded for comparison using a SiLi detector positioned at 135° detection angle. The conventional RBS spectra were analyzed using simulations with the SIMNRA software package [20].

To determine deposition sequences, combinations of two different inks were deposited in a document such that the inks intersect at some points using laser printers/inkjet printer/gel pen/ballpoint pen. Subsequently to deposition, the samples were mounted on a sample holder to perform micro-RBS and micro-PIXE at the intersection of the inks. In the experiment, 2 MeV He ions were directed to the sample at normal incidence and the backscattered He were detected using an SSD detector with scattering angle of 168.5°. The ions with typical beam currents of 100 pA were focused to a beam spot size of a few micrometers using a triple magnetic quadrupole lenses. The typical size of the ion beam spot was 6 × 4 μm which was confirmed by scanning the ions over a Cu-TEM grid. Since the ion beam resolution is sufficient for the analysis of the inks, the He ions were scanned on samples and the RBS and PIXE spectra were recorded. RBS and PIXE 2D maps were obtained from energy-resolved backscattering yields and X-ray yields.

3 | RESULTS AND DISCUSSIONS

Experimental and simulated RBS and experimental PIXE spectra of plain paper and inks are shown in Figure 1. The projected range of 2 MeV He ions is around 15 μm in the paper/inks if the concentration of H was assumed to be 50 at.% and the density of paper to be 0.75 g/cm^3. With 2 MeV He ions, RBS spectra were obtained containing information from the target surface to approximately 6 μm depth. The characteristic X-rays excited in the targets and recorded in the PIXE detector can have a larger range; however, as excitation cross sections decrease with decreasing energy, approximately similar average sampling depth can be assumed. RBS simulations fitted to the experimental data were, when necessary, performed assuming several layers with various composition. The composition of the samples is obtained by RBS simulations with the exception of hydrogen (H is undetectable from RBS) and the resulting bulk composition, is shown in Table 1. However, the composition of the top surface (900–1800 × 10^{15} atoms/cm^2) is found different from this value for all the samples. We also find, that (except thin layer at surface), the concentration of carbon is higher than that of plain paper in all investigated inks. The concentration of oxygen is found lower than in plain paper in all the inks/toner. Ca, used as a bleaching agent, is the heaviest element expected in the plain paper detectable by conventional RBS. The measured Ca concentration is reduced drastically in laser print 1 and laser print 2 compared with plain paper. A significant decrease in Ca concentration is observed in all the inks compared with plain paper. Analyzing plain samples of the different coloring agents, in laser print 1, the heaviest element observed by RBS is Fe (Fe edge can be seen clearly in Figure 1A). From the RBS simulations, the depth distribution of Fe was analyzed, and from simulation (shown in Figure 1), ~7% of Fe is found throughout the sample depth analyzed by RBS. Thus, the thickness of deposited toner is expected to be up to a few microns. Altogether, these results show that the different inks and toners have significantly different properties when casted on paper. While laser printers may deposit toners on the surface of the material, inkjet ink and gel pen are water-based writing tools and therefore are completely soaked into the paper which can induce gradients in composition over several μm until bulk composition is reached.

As discussed earlier, the composition is uniform in the probed depth range except for a thin surface layer in all samples. Particularly, concentrations of heavy elements are found slightly lower in a thin surface layer compared with larger depth. For example, in laser print 1, the Fe concentration is lower (on average ~5 at.%) at the thin surface layer (1400 × 10^{15} atoms/cm^2) compared with higher depth (~7 at.%). In the RBS spectrum obtained for laser print 2, a signal due to Ti can be observed in both RBS and PIXE. Different from the laser print 1, Ti is clearly present in a very thin layer on the surface only (thickness is 300 × 10^{15} atoms/cm^2 and composition is ~1%). From RBS simulations, significant portion of Si is found on the top of the paper/ink and the other light elements may be penetrated bit deeper into paper in laser print 2. In the ballpoint pen, gel pen, and inkjet, the Ca concentration is decreased by ~0.5 at.% at the surface (thickness of 1200, 1800, 900 × 10^{15} atoms/cm^2, respectively) compared with larger depths. Thus, these inks are expected to at least partially penetrate the paper. This result shows that RBS can yield additional complementary information on inks deposited from the acquired depth profile for both ink and paper constituents.

In the following, different combinations of coloring agents are analyzed using micro-RBS and micro-PIXE imaging as shown in Figure 2A. For the combination of the two laser printers, in agreement with the data from conventional RBS obtained for plain samples as discussed before, the Fe signal is dominant in laser print 1 while the total number of counts in laser print 2 is lower than that of plain paper. Thus, the signal from laser print 1 appears very pronounced while laser print 2 appears to be less intense in the total RBS image (shown in Figure 2A). Note, that, this discrimination is not apparent in the total PIXE image, as the majority of the signal originates from Ca, as apparent from Figure 1. Element-specific micro-RBS and micro-PIXE by selecting a specific energy range from PIXE and RBS spectra can permit further discrimination of inks. For example, a map for the spectral region associated exculsively with Fe (Fe-RBS) is obtained by integrating the RBS spectrum from 1400 to 1500 keV while a corresponding map of the signal associated with iron in PIXE (Fe-PIXE) results from integrating the spectrum from 5.5 to 7 keV. Thus, the ion beam techniques are more effective if the ink contains heavy elements such as Fe and Ti. Even though the laser print 2 contains Ti, it is not seen in micro-RBS and micro-PIXE due to its very low concentration and may be observed only upon increasing measurement time. The Ca-PIXE maps show suppression of Ca counts in both inks while the Si-PIXE maps shows an increase in Si counts compared with plain paper.

Figure 2A shows the optical image, total RBS map, Fe-RBS map, and Fe-PIXE maps for the sample where laser print 2 is on the top of laser print 1. The total RBS map shows a clear gap/

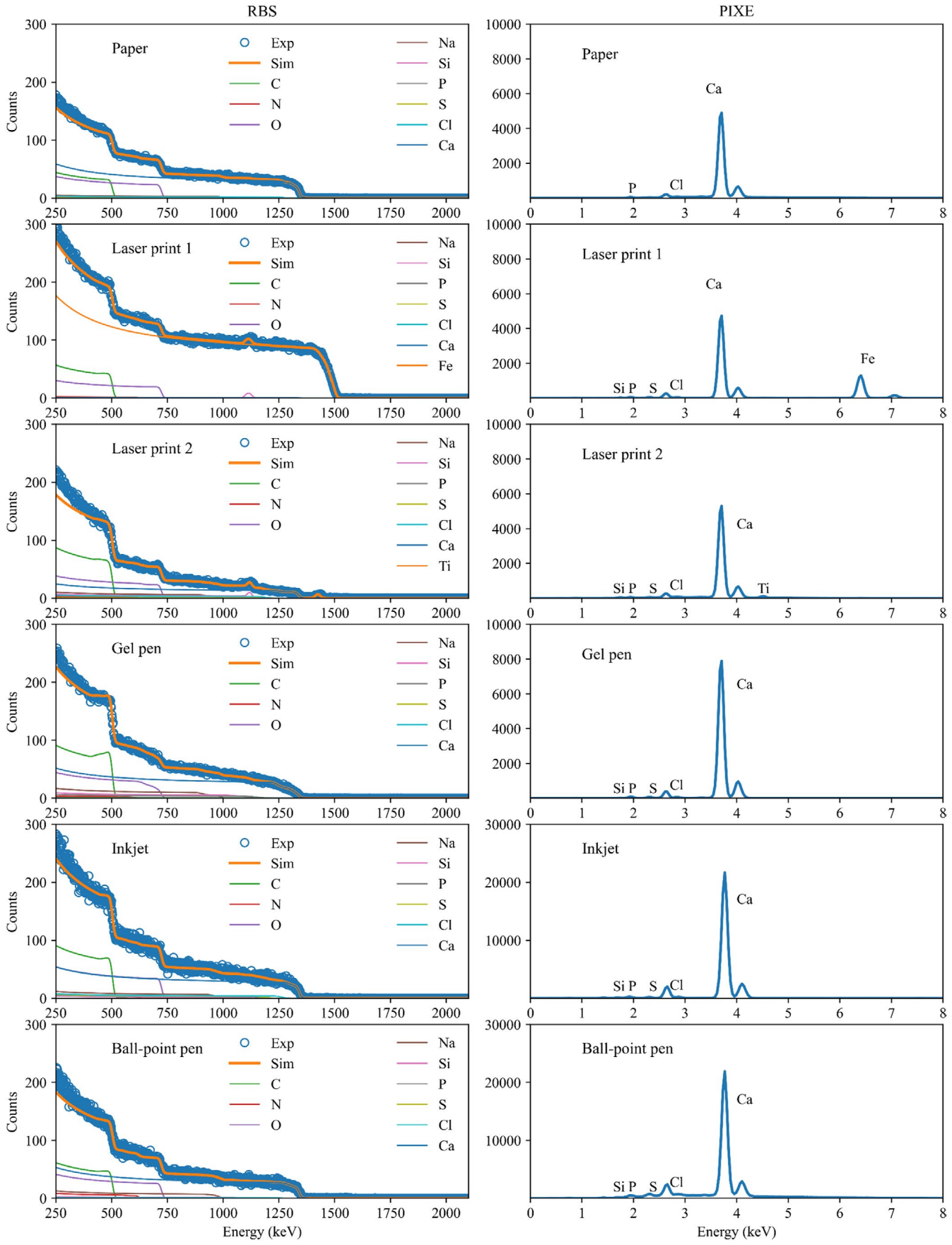

FIGURE 1 Experimental and simulated conventional RBS spectra (left) and conventional PIXE spectra (right) of paper and inks deposited on paper [Colour figure can be viewed at wileyonlinelibrary.com]

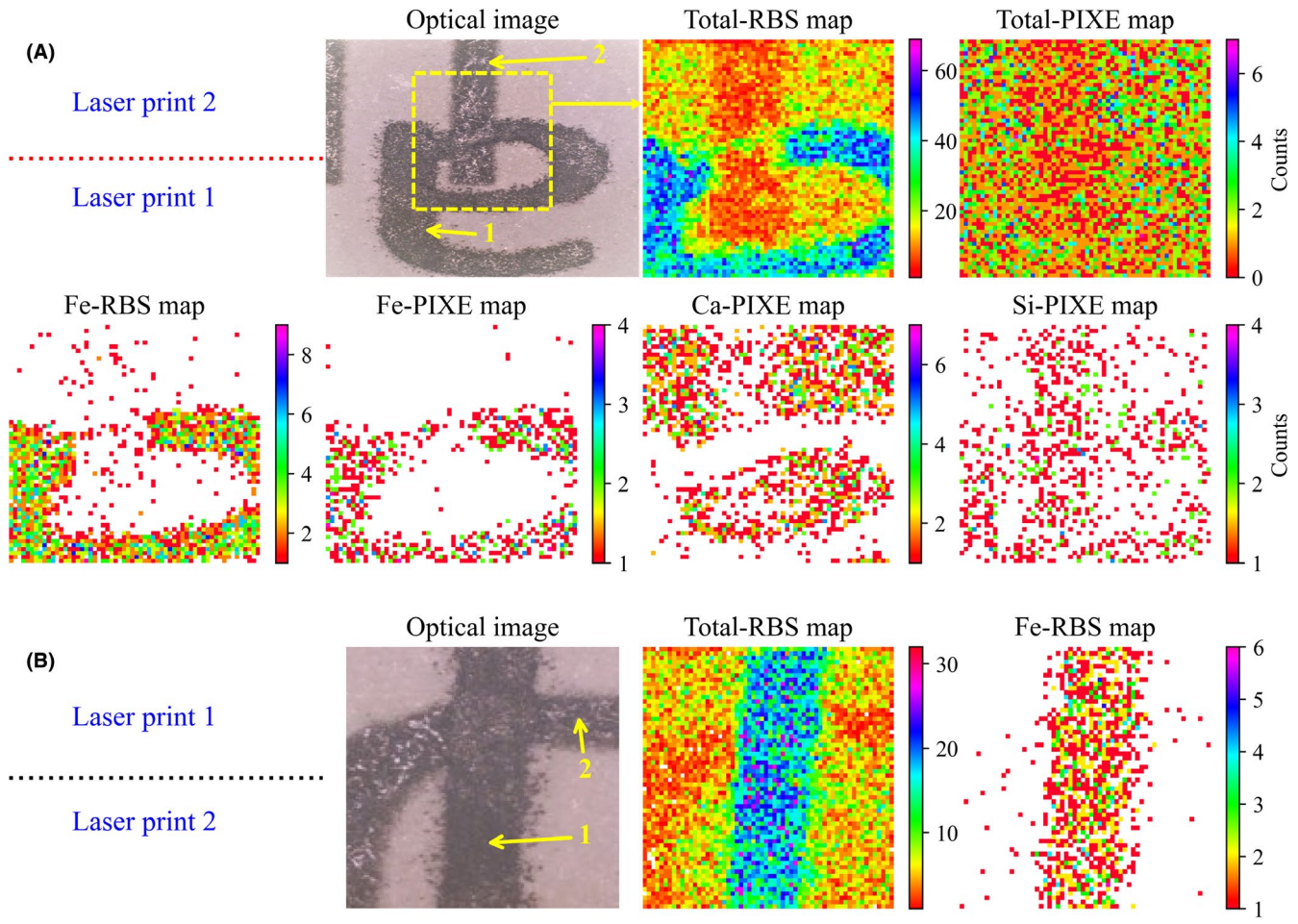

FIGURE 2 Optical images of the sample region in which micro-RBS and micro-PIXE performed are shown together with total and element-specific RBS and PIXE maps of overlapping inks for (A) laser print 2 deposited on laser print 1 and (B) laser print 1 deposited on laser print 2. These two laser toners are clearly seen from total RBS maps in both samples. One staining agent shows continuity while the other one shows a gap at the intersection, from which the order of deposited inks is directly identified [Colour figure can be viewed at wileyonlinelibrary.com]

discontinuity for laser print 1 and continuity for laser print 2 in this sample. The Fe-RBS maps also shows a clear gap for laser print 1. So, the RBS correctly predict that the laser print 1 ink is deposited first. In comparison, the PIXE map for Fe shows only a weak discontinuity for laser print 1. Thus, RBS signals are superior to PIXE maps for this analysis due to the availability of depth-resolved element information. The sample where laser print 1 is on the top of laser print 2 is shown in Figure 2B. Total RBS map and Fe-RBS map show continuity for laser print 1 and discontinuity for laser print 2. From this analysis, the laser print 2 is found to be deposited first in the document. Thus, our micro-RBS analysis correctly predicts the chronology of intersecting inks for the combinations of laser print 1 and laser print 2 toners.

Figure 3A shows the optical image, total and Fe-RBS image for the sample where gel pen ink is deposited on the top of laser print 1. The Fe-RBS map shows a clear gap in the signal associated with laser print 1. Different from the previous case, however, where both agents resulted in an increase or suppression of the signal in the total RBS map, the gel pen ink was not distinguishable clearly from the signal by plain paper in the total RBS map. However, in agreement with conventional RBS, the Ca signal is slightly decreased in gel pen compared with plain paper (see Ca-PIXE map in Figure 3A). Thus, for the integral intensity the only possibility of deducing the deposition sequence is based on changes in the signal of laser print 1. In agreement with total RBS map, the Fe-RBS map shows a clear gap for laser print. Note, however, that the gap in the signal is narrower than the visible track of deposited ink. One possible explanation for this observation would be mechanical scratching of the toner from laser print 1 by the gel pen. Note, that in Fe-PIXE maps, the gap is not clearly seen due to poor statistics. Again, the PIXE maps are less effective than RBS maps for finding the order of deposited inks in this document. Based on the gap observed in the laser print 1, one can conclude that the laser print 1 is deposited first. Figure 3B shows the optical image, total, and Fe-RBS image for the sample where laser print 1 is deposited on the top of pen ink. The total RBS maps and Fe-RBS maps show continuity for laser print 1. Since the pen ink is not visible, we conclude, based only on the continuity of laser print toner in the document, the laser print 1 is on the top of the pen ink. Thus, our analysis correctly predicts the order of deposition of inks for the combinations of laser print 1 and pen ink.

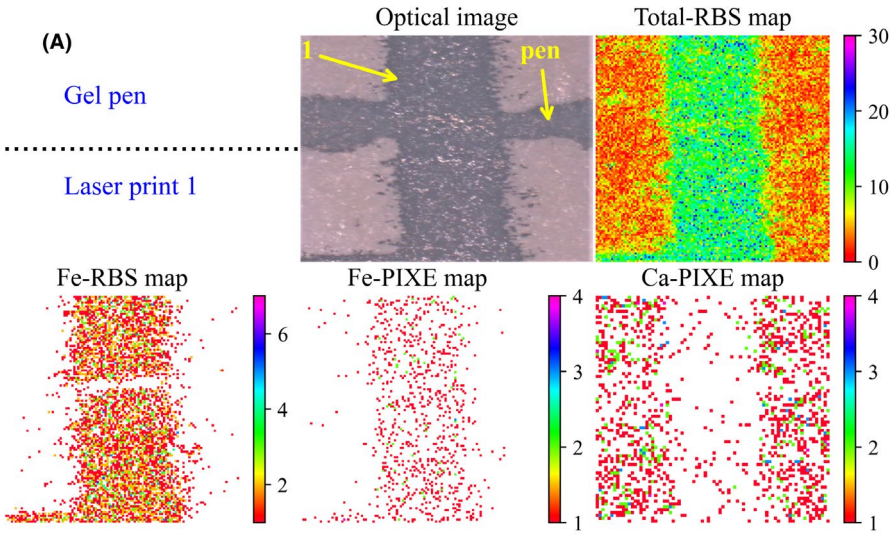

FIGURE 3 Optical image and total RBS, Fe-RBS, Fe-PIXE, and Ca-PIXE maps of overlapping inks (A) gel pen on top of laser print 1 and (B) laser print 1 on top of gel pen. Gel pen is not visible in the total RBS maps while laser print 1 is seen. However, a small gap is observed in Fe-RBS maps for gel pen on top of laser print 1, while Fe-PIXE map show no gap [Colour figure can be viewed at wileyonlinelibrary.com]

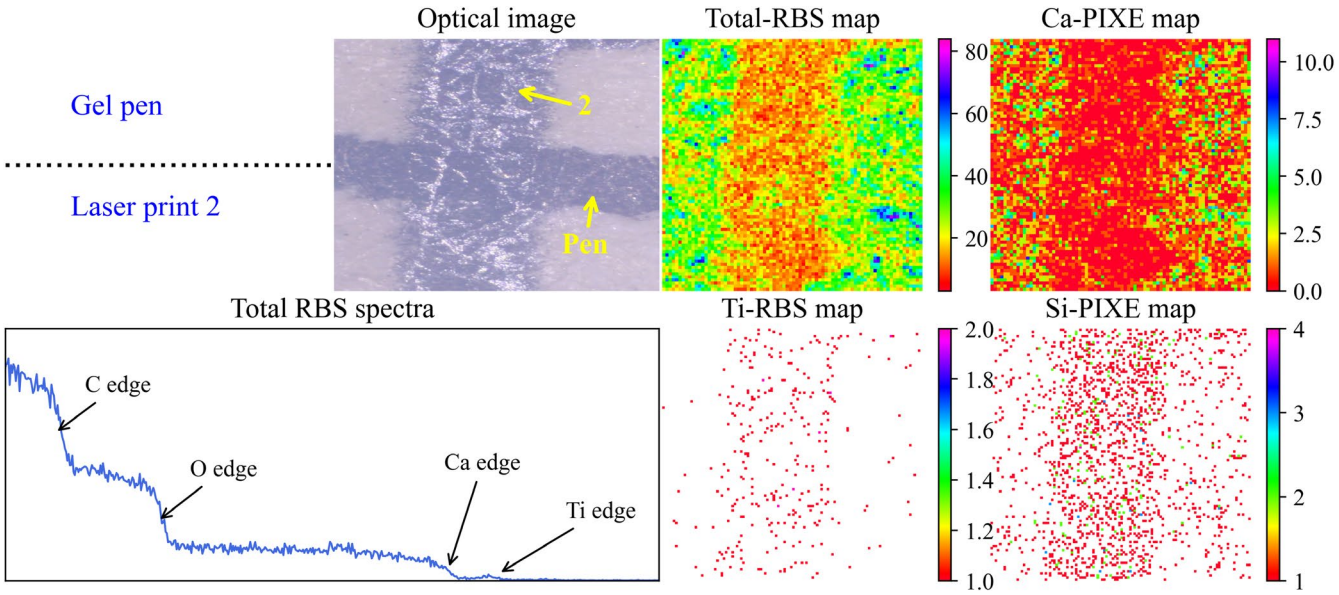

FIGURE 4 Optical image and total RBS, Ti-RBS, Si-PIXE, and Ca-PIXE maps of overlapping inks—gel pen on top of laser print 2. The total RBS spectrum is shown and a small peak due to Ti is seen from laser print 2 [Colour figure can be viewed at wileyonlinelibrary.com]

Note, however, that the condition of an RBS spectrum being distinct from plain paper does not necessary suffice for resolving deposition sequence. As an example, we present an analysis for both the gel pen and toner 2, which feature both RBS spectra quite distinct from plain paper, but qualitatively similar to each other. Optical image and total RBS, Ti-RBS, Si-PIXE, and Ca-PIXE maps of gel pen on top of laser print 2 is shown in Figure 4. Small Ti peak was observed from total RBS spectrum. Since the Ti is from laser print 2 (known from conventional RBS and PIXE), the Ti-RBS map can be used to find the order of deposition. The laser print 2 is seen from total RBS and Si-PIXE and Ti-RBS maps. But the expected gap is not observed in all the maps. The gel pen ink may be penetrated into the laser print ink 2 and finding the sequence of deposition is difficult with the present statistics.

Finding the deposition sequence of the inkjet, and ball-point pen inks is expected to be most challenging due to the similarity in RBS spectra. They are thus expected to be not visible in total RBS as the expected yield per incident charge is similar to that of the plain paper (compare Figure 1). So, the analysis for finding the order of deposition is difficult with present methods for combinations of these inks. However, these inks in combination with laser print inks may be studied as laser print inks showed distinct RBS spectra and feature a different yield/charge in the total RBS maps.

As an example, the combination of laser print 1 and inkjet ink was studied and the total RBS, Fe-RBS, total PIXE, and Fe-PIXE maps are shown in Figure 5. No gap was observed at the intersection of inkjet ink deposited on top of laser print 1 in RBS and PIXE maps. As discussed earlier, inkjet and ballpoint pen agents are soaked into paper and also expected to penetrate deep into the toner deposited by laser print 1. Thus, both the PIXE and RBS maps fail to show a gap at the intersection and finding the order of deposition for inkjet inks is difficult irrespective of the other agent.

Figure 6 shows the total RBS, Fe-RBS, total PIXE, and Fe-PIXE maps of samples with combinations of ball-point pen ink and laser print 1. A gap may be expected for laser print 1 in total RBS maps in the case of ball-point pen ink deposited on top of laser print 1. Such a gap could result from scratching the earlier deposited toner, in analogy to the gel pen, as well as a dilution of the Fe, in case the ink is penetrating the toner, in both cases resulting in reduced counts from the intersection of inks compared with laser print 1. However, no gap is observed in RBS and PIXE maps. Note, however, that a weak trace aligned with the track of the ballpoint pen can be detected in the Fe-RBS maps, which can be potentially be explained by picking up traces of toner by the ball point. While from the toner signal, the deposition sequence is difficult to determine, potential redeposition of chemical species only present in one agent can be another hint on the deposition sequence.

Finally, for illustrating the potential for reconstruction of a hidden text in a document, Laser print 1 is printed first in a test document and then printed letters are shadowed by ball-point pen. The RBS map was obtained from the shadowed area in the sample and shown in Figure 7. From the total RBS map, the printed line is clearly discriminated from ball-point pen ink (shown in Figure 7) whereas the total PIXE map shows no difference between the two inks. One can also use the Fe-RBS, Fe-PIXE, and Ca-PIXE signals for discrimination of inks. Thus, micro-RBS/PIXE could be used to reconstruct the hidden text in a questioned document.

4 | CONCLUSION

The present study illustrates that Rutherford Backscattering Spectrometry performed with high spatial resolution can be a complementary tool for reconstruction of the deposition sequence of inks in questioned documents. The depth-resolved information on sample composition can, in certain cases, be decisive for reconstructing the specific deposition sequence. In general, we obtained similar qualitative information when comparing particle-induced X-ray Emission and RBS, further confirming the potential of ion beam-based methods for the present kind of forensic analysis. Specifically, it could be shown that the presence of heavier elements in the staining agent makes analysis possible. Also, near-surface

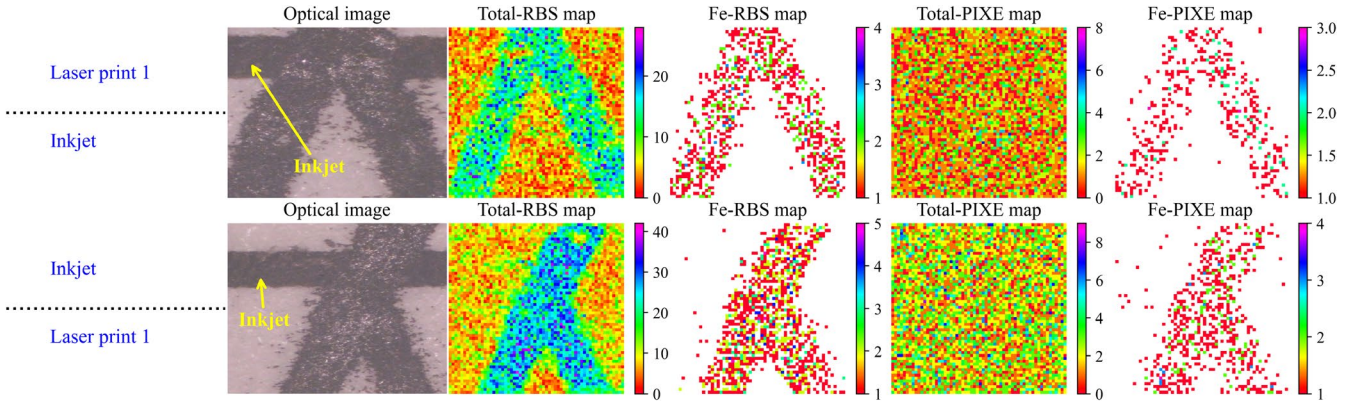

FIGURE 5 Optical image and total RBS, Fe-RBS, total PIXE, and Fe-PIXE maps of overlapping inks, (i) laser print 1 on top of inkjet ink and (ii) inkjet ink on top of laser print 1. No gap is seen from total RBS, Fe-RBS, total PIXE, and Fe-PIXE maps due to penetration of inkjet ink into the other ink [Colour figure can be viewed at wileyonlinelibrary.com]

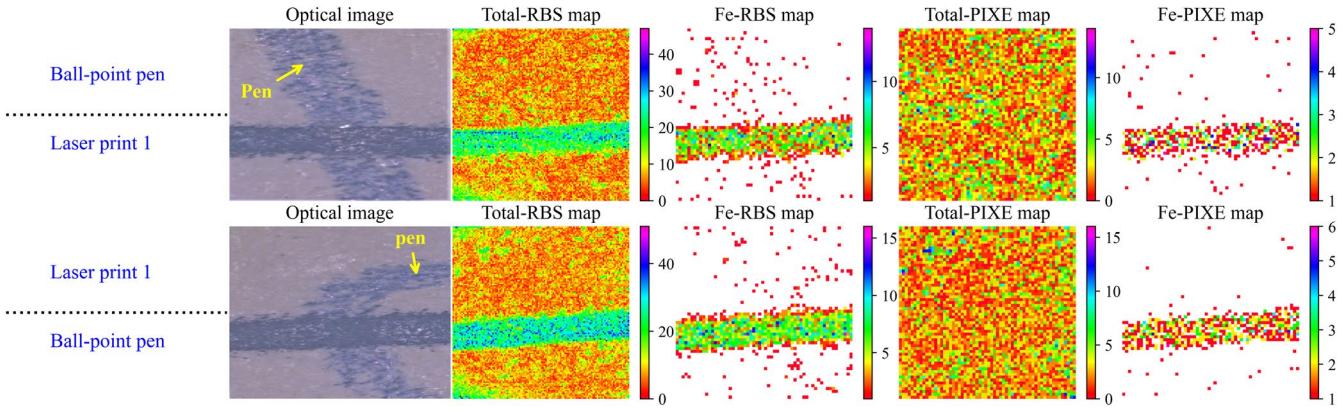

FIGURE 6 Optical image and total RBS, Fe-RBS, total PIXE, and Fe-PIXE maps of overlapping inks of ball-point pen and laser print 1 [Colour figure can be viewed at wileyonlinelibrary.com]

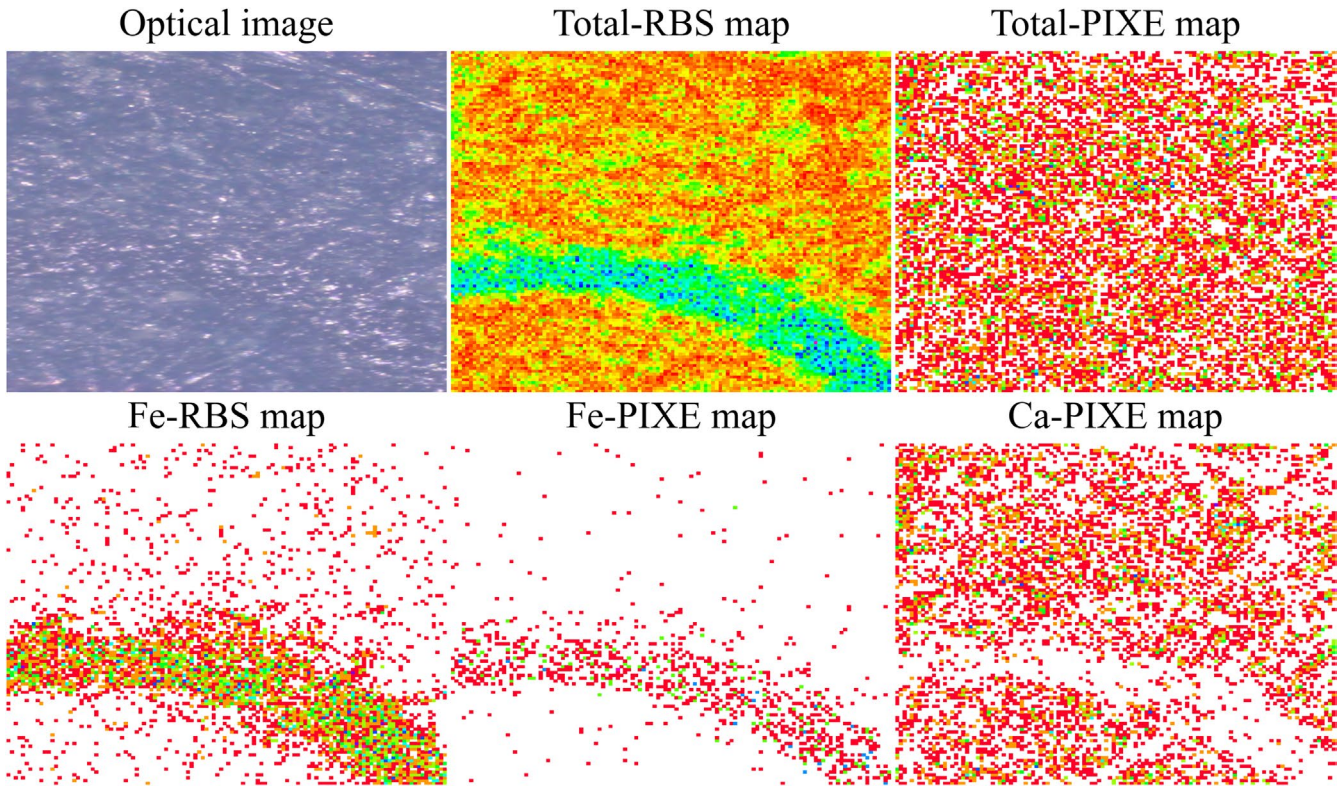

FIGURE 7 Optical image, total RBS, total PIXE, Fe-RBS, Fe-PIXE, and Ca-PIXE maps of document where laser print 1 is deposited first and later a ball-point pen was employed to obscure the character [Colour figure can be viewed at wileyonlinelibrary.com]

deposition, such as for laser toners, is advantageous. In contrast, for writing tools which are water-based organic materials and penetrate deep into the paper or which only feature very low concentration of heavy elements, analysis is hampered. Employing ion beams with lower energy can help to partially overcome this issue, while techniques with higher sensitivity to light elements might be superior.

ORCID

Vairavel Mathayan https://orcid.org/0000-0002-5820-2807

REFERENCES

1. e Brito LR, Martins AR, Braz A, Chaves AB, Braga JW, Pimentel MF. Critical review and trends in forensic investigations of crossing ink lines. Trends Analyt Chem. 2017;94:54–69. https://doi.org/10.1016/j.trac.2017.07.005.
2. Strach SJ. Establishing the sequence of intersecting ballpoint pen strokes. Forensic Sci. 1978;11:67–74. https://doi.org/10.1016/0379-0738(78)90094-4.
3. Claybourn M, Ansell M. Using Raman spectroscopy to solve crime: inks, questioned documents and fraud. Sci Justice. 2000;40:261–71. https://doi.org/10.1016/S1355-0306(00)71996-4.

4. Braz A, López-López M, García-Ruiz C. Raman spectroscopy for forensic analysis of inks in questioned documents. Forensic Sci Int. 2013;232:206–12. https://doi.org/10.1016/j.forsciint.2013.07.017.
5. Braz A, López-López M, García-Ruiz C. Raman imaging for determining the sequence of Ball-point pen ink crossings. Forensic Sci Int. 2015;249:92–100. https://doi.org/10.1016/j.forsciint.2015.01.023.
6. Silva CS, Pimentel MF, Honorato RS, Pasquini C, Prats-Montalbán JM, Ferrer A. Near infrared hyperspectral imaging for forensic analysis of document forgery. Analyst. 2014;139:5176–84. https://doi.org/10.1039/C4AN00961D.
7. de Morais DR, de Morais CJ, Razzo D, Eberlin MN, Costa JL, Santos JM. Forensic determination of crossing lines involving stamp and pen inks by mass spectrometry imaging. Anal Methods. 2020;12:951–8. https://doi.org/10.1039/C9AY02330E.
8. Chen S-Z, Tsai T-L, Chen Y-F. Forensic application of atomic force microscopy – Questioned document. J Chin Chem Soc. 2012;59:283–8. https://doi.org/10.1002/jccs.201100739.
9. Lee KY, Lee J, Kong SG, Kim B. Sequence discrimination of heterogeneous crossing of seal impression and ink-printed text using adhesive tapes. Forensic Sci Int. 2014;234:120–5. https://doi.org/10.1016/j.forsciint.2013.11.003.
10. Dirwono W, Park JS, Agustin-Camacho MR, Kim J, Park H-M, Lee Y, *et al*. Application of micro-attenuated total reflectance FTIR spectroscopy in the forensic study of questioned documents involving red seal inks. Forensic Sci Int. 2010;199:6–8. https://doi.org/10.1016/j.forsciint.2010.02.009.
11. Almeida CM, Sales DD, Tosato F, dos Santos NA, Filho JFA, Macrino CJ, *et al*. Study of chemical profile and of lines crossing using blue and black ink pens by LDI (+) MS and LDI (+) imaging. Microchem J. 2019;148:220–9. https://doi.org/10.1016/j.microc.2019.05.002.
12. Kim J, Kim M, An J, Kim Y. Determination of the sequence of intersecting lines using Focused Ion Beam/Scanning Electron Microscope. J Forensic Sci. 2016;61:803–8. https://doi.org/10.1111/1556-4029.13076.
13. He A, Karpuzov D, Xu S. Ink identification by time-of-flight secondary ion mass spectroscopy. Surf Interface Anal. 2006;38:854–8. https://doi.org/10.1002/sia.2246.
14. Bright NJ, Webb RP, Bleay S, Hinder S, Ward NI, Watts JF, *et al*. Determination of the deposition order of overlapping latent fingerprints and inks using secondary ion mass spectrometry. Anal Chem. 2012;84:4083–7. https://doi.org/10.1021/ac300185j.
15. Goacher RE, DiFonzo LG, Lesko KC. Challenges determining the correct deposition order of different intersecting black inks by time-of-flight secondary ion mass spectrometry. Anal Chem. 2017;89:759–66. https://doi.org/10.1021/acs.analchem.6b03411.
16. Moore KL, Barac M, Brajković M, Bailey MJ, Siketić Z, Radović IB. Determination of deposition order of toners, inkjet inks, and blue ballpoint pen combining MeV-secondary ion mass spectrometry and particle induced X-ray emission. Anal Chem. 2019;91:12997–3005. https://doi.org/10.1021/acs.analchem.9b03058.
17. Tesmer JR, Nastasi M, Barbour JC, Maggiore CJ, Mayer JW. Handbook of ion beam analysis. Pittsburgh, PA: Materials Research Society, 1995; p. 64–77.
18. Mayer J, Rimini E, eds. Ion handbook for material analysis. New York, NY: Academic Press, 1977; p. 55–60.
19. Primetzhofer D, Bauer P. Trace element quantification in high-resolution Rutherford backscattering spectrometry. Nucl Instru Meth B 2011;269:1284–7. https://doi.org/10.1016/j.nimb.2010.11.028.
20. Mayer M. SIMNRA, a simulation program for the analysis of NRA, RBS and ERDA. AIP Conf Proc. 1999;475:541–4. https://doi.org/10.1063/1.59188.

How to cite this article: Mathayan V, Sortica M, Primetzhofer D. Determining the chronological sequence of inks deposited with different writing and printing tools using ion beam analysis. *J Forensic Sci*. 2021;66:1401–1409. https://doi.org/10.1111/1556-4029.14705